



# A PHYSICAL EXPLANATION FOR THE EFFECTIVENESS OF PLANET PHASING TO SUPPRESS PLANETARY GEAR VIBRATION

ROBERT G. PARKER

*Department of Mechanical Engineering, The Ohio State University, 206 W. 18th Ave., Columbus, OH 43210-1107, U.S.A.*

*(Received 18 June 1999, and in final form 2 December 1999)*

The effectiveness of planet phasing to suppress planetary gear vibration in certain harmonics of the mesh frequency is examined based on the physical forces acting at the sun–planet and ring–planet meshes. The analysis does not rely on assumptions of the nature of the dynamic excitation (e.g., static transmission error or time-varying mesh stiffness) or on an underlying dynamic model. Instead, the inherent system symmetries imply distinct relationships between the forces at the multiple meshes. These relationships lead naturally to simple rules for when a particular harmonic of mesh frequency is suppressed in the dynamic response. An important implication is that certain expected resonances when a mesh frequency harmonic and a natural frequency coincide are suppressed. Systems with equal planet spacing and those with unequally spaced, diametrically opposed planets are considered. In both cases, a substantial number of mesh frequency harmonics are suppressed naturally without optimization of the phasing. The phenomena are demonstrated with a dynamic finite element/contact mechanics simulation. © 2000 Academic Press

## 1. INTRODUCTION

The dynamic response of planetary gears (Figure 1) is of fundamental importance in helicopters, automotive transmissions, aircraft engines, and a variety of industrial machinery. The complex, dynamic forces at the sun–planet and ring–planet meshes are the source of the vibration. Modelling of the dynamic tooth forces remains an important issue that has not been resolved even for single-mesh gear pairs. The multiple meshes of planetary gears further complicate the dynamic modelling. Consequently, dynamic analyses of planetary gears are less developed than for other single-mesh gear configurations. In particular, experimental verification of the existing analytical models is especially limited. As a result, design options to minimize noise and loads in planetary gears have developed empirically without strong analytical or experimental foundation. These design strategies include tooth-shape modifications, gear geometry adjustments (pitch, contact ratio, etc.), reduction of manufacturing tolerances, use of “floating” sun, ring, or carrier components, and vibration isolation concepts. A particular strategy is the use of *planet phasing*, where the planet configuration and tooth numbers are chosen such that self-equilibration of the mesh forces reduces the net forces and torques on the sun, ring, and carrier, thereby reducing vibration. This idea was proposed by Schlegel and Mard [1] where experimental measurements on a spur gear system demonstrated a noise reduction of 11 dB. Seager [2] gave a more detailed analysis using a static transmission error model of the dynamic excitation. Palmer and Fuehrer [3] also demonstrate the effectiveness of planet phasing and support their arguments with limited experiments. Kahraman [4] and Kahraman and

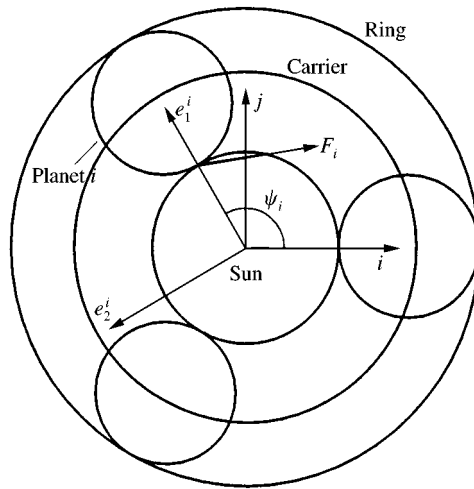


Figure 1. Planetary gear schematic.  $F_i$  denotes the mesh force at the  $i$ th sun-planet mesh.

Blankenship [5] studied the use of planet phasing in the context of helical planetary systems. These works use the static transmission error to represent the dynamic excitation in a lumped parameter dynamic model. All of these studies focus on planetary gears with equally spaced planet gears. Platt and Leopold [6] measured noise reductions for a particular helical gear design as a result of different phasing designs; no analysis is presented.

The purpose of this work is to examine the analytical basis for planet phasing in spur planetary systems and to extend the concept to systems with unequal planet spacing. The results are developed in terms of the physical mesh forces and are not tied to any lumped-parameter model. In fact, no attempt is made to characterize the factors affecting the mesh forces (tooth-bending interactions, profile modifications, contact pressure, etc.) or quantify their magnitudes. The fundamental issue is that the inherent symmetries of the planetary design imply distinct relationships between the dynamic forces at the individual meshes. This approach seems more appealing to physical intuition and makes no supposition about the use of static transmission error to model the dynamic excitation. These symmetries lead naturally to specific conclusions for the suppression of particular harmonics of mesh frequency in the net forces and torques on the sun, ring, and carrier. Simple rules (with clear design application) emerge to suppress expected resonances that occur when the mesh frequency  $\omega_m$  or one of its harmonics ( $l\omega_m$ ,  $l = 1, 2, 3, \dots$ ) coincides with a system natural frequency.

The unique structure of planetary gear vibration modes is essential in what follows. Planetary gears with equal sun-planet mesh stiffness at each mesh, equal ring-planet mesh stiffness at each mesh, and equal planet inertia properties have exactly three types of modes for systems with equally spaced or diametrically opposed planets [7, 8]:

- (1) *Translational modes* in which the sun, ring, and carrier have only translational motion and no rotational motion.
- (2) *Rotational modes* in which the sun, ring, and carrier have only rotational motion and no translational motion.
- (3) *Planet modes* in which the sun, ring, and carrier have no motion and only the planets deflect. These exist only for four or more planets.

TABLE 1

*Natural frequencies of the four and three planet gear systems*

Natural frequency (Hz)	Mode type					
	Translation	Rotation	Planet	Tanslation	Rotation	Translation
Four planets	778	1144	1729	1676	1723	2110
Three planets	780	1104		1695	1743	2145

## 2. TWO EXAMPLES

To motivate the subsequent analysis, the phenomena are demonstrated first using two examples. The results show how certain modes of a planetary gear are excited to resonance while others are seemingly immune to resonant excitations. The findings in this section are from a finite element simulation. In the following section, the computed results are explained analytically based on symmetry arguments independent of any mathematical model or computational simulation. The examples are based on the four and three planet configurations of the U.S. Army OH-58 helicopter planetary gear. The system is described in detail in Krantz [9] and Parker *et al.* [10], where a comprehensive study of the dynamic response is conducted. Importantly, nothing in the finite element simulation predisposes the dynamic response to the peculiar behavior described below. In particular, no *a priori* assumptions are made regarding the spectral content of the dynamic mesh forces; these are determined by contact analysis at each mesh at each time step. Specifically, idealizations of the dynamic excitation in terms of static transmission error or a specified time-varying mesh stiffness are not used.

### 2.1. FOUR PLANET SYSTEM

The four planet configuration has unequally spaced planets at the angular orientations  $\psi_i = 0, 91.4, 180, \text{ and } 271.4^\circ$ . The sun, planet, and ring have the numbers of teeth  $Z_s = 27$ ,  $Z_p = 35$ , and  $Z_r = 99$ . The natural frequencies are given in Table 1. Figure 2 shows the spectrum of the steady state planet radial deflection for a range of operating speeds. At all speeds, the response has frequency content only at mesh frequency and its harmonics, although this is not imposed in the finite element model. Resonant response in the first mode ( $f_1 = 778$  Hz), a translational mode, is evident when the mesh frequency or any of its *odd* harmonics coincide with  $f_1$ . Expected resonances when *even* harmonics of mesh frequency coincide with  $f_1$  are absent. Similar behavior occurs for the translational mode with natural frequency  $f_6 = 2110$  Hz. In contrast, resonant response in the second mode ( $f_2 = 1144$  Hz), a rotational mode, is evident when the mesh frequency or any of its *even*, but not *odd*, harmonics coincide with  $f_2$ . (The resonance excited by the fourth harmonic at mesh frequency  $f_m = 286$  Hz is small but present. Refined increments of mesh frequency in the simulation would make this more apparent.) Similar behavior for modes 3–5 cannot be distinguished because of the proximity of their natural frequencies. Analogous figures for sun translation and rotation [10] show that sun translation has no spectral content in the *even* harmonics of mesh frequency, and rotational mode resonances are absent in the remaining odd harmonics. The sun rotational response has no spectral content in the *odd* harmonics of mesh frequency, and translational mode resonances are absent in the remaining even harmonics.

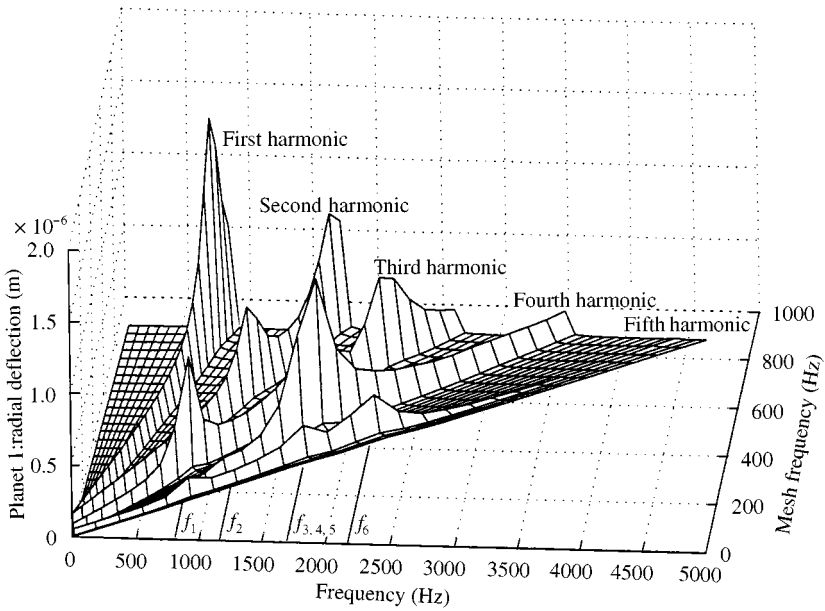


Figure 2. Steady state planet radial displacement spectrum for a range of operating speeds for the four planet system.  $f_i$  denotes the  $i$ th natural frequency. Harmonics of the mesh frequency are indicated.

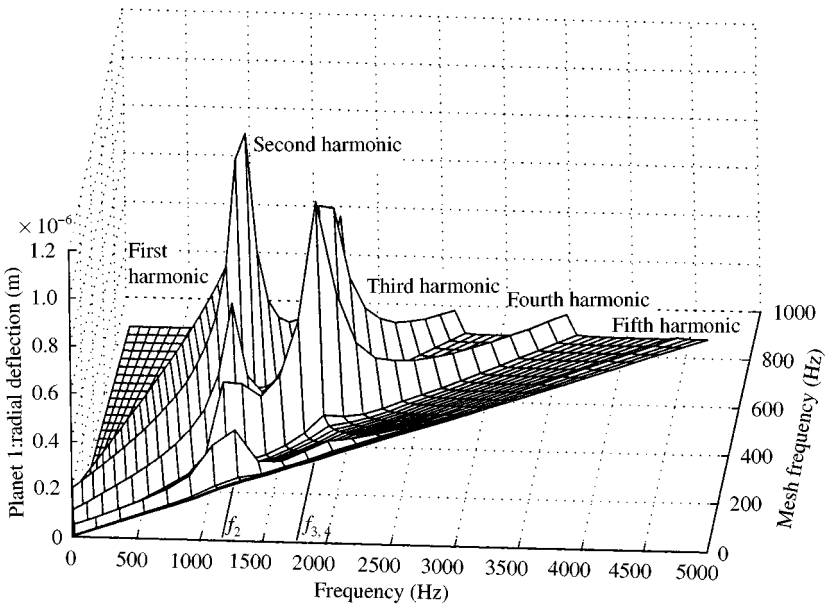


Figure 3. Steady state planet radial deflection spectrum for a range of operating speeds for the three planet system.  $f_i$  denotes the  $i$ th natural frequency. Harmonics of the mesh frequency are indicated.

## 2.2. THREE PLANET SYSTEM

The three planet configuration uses identical sun, ring, and planet gears as the four planet system. In contrast to the four planet case, the three planets are equally spaced. Natural frequencies are given in Table 1. Figure 3 shows the steady state dynamic response of the

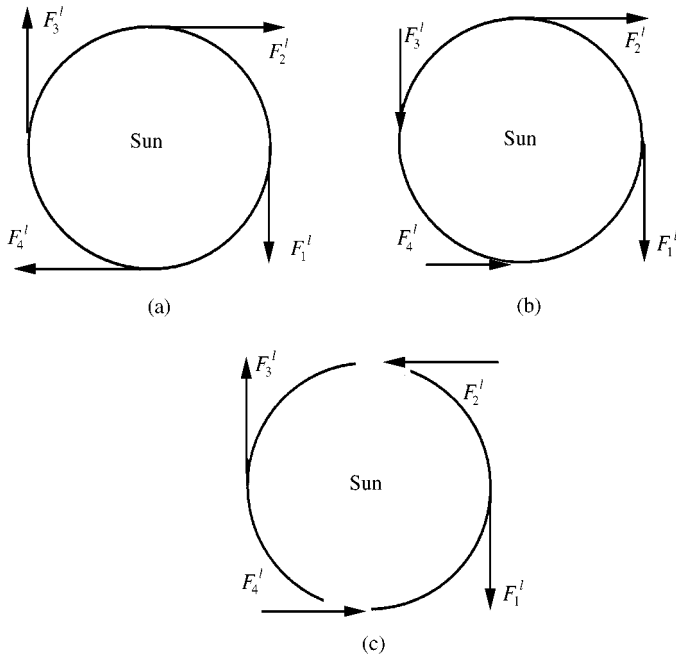


Figure 4. Representative forces acting on the sun gear in the  $l$ th harmonic of mesh frequency. (a) Forces cancel, torques add; (b) Forces add, torques cancel; (c) Forces cancel, torques cancel.

planet radial deflection. The translational modes ( $f_1 = 780$  and  $f_5 = 2145$  Hz) are not excited to resonance by *either* odd or even harmonics of mesh frequency at any speed. The rotational modes ( $f_2 = 1104$  and  $f_4 = 1743$  Hz), however, are excited to resonance at the speeds  $lf_m = f_2$  for any integer mesh frequency harmonic  $l$ . Corresponding results for the sun [10] show that its rotation has spectral content in all mesh frequency harmonics, but the sun translation is always zero at all speeds.

### 3. MESH FORCE ANALYSIS

In general, resonance corresponding to a natural frequency  $f_n$  is excited in the  $l$ th mesh frequency harmonic at a mesh frequency of  $f_m = f_n/l$ . The above behavior wherein resonances at certain natural frequencies occur at particular mesh frequency harmonics and are absent from other mesh frequency harmonics is explained by a mesh force analysis. These relationships predict whether or not a particular type of mode (translational or rotational) is excited in a given mesh frequency harmonic.

The basic phenomenon is illustrated in the sketch of Figure 4, which shows three possibilities for the force distribution in a four planet system. Note that the forces shown are the  $l$ th mesh frequency harmonic in the Fourier decomposition of the dynamic mesh force. In Figure 4(a), the  $l$ th harmonic of the net mesh force/torque on the sun induces rotational motion of the sun at the frequency of the  $l$ th harmonic but not translation. In Figure 4(b), the  $l$ th harmonic of the net mesh force/torque on the sun induces translational motion of the sun but not rotation. For the case of Figure 4(c), the  $l$ th harmonic of the net sun force and moment vanish and no sun motion occurs in the  $l$ th harmonic. Conditions for which these three behaviors occur for a particular mesh frequency harmonic are derived analytically below.

The complex tooth meshing action results in dynamic forces acting on the sun and ring gears from the planet meshes. (For concreteness, the following discussion examines sun forces, though the analysis for ring forces is analogous.) These forces are periodic functions with the fundamental frequency equal to the tooth mesh frequency  $\omega_m = 2\pi f_m$ . The force acting on the sun gear at the  $i$ th planet mesh (Figure 1) is expressed using a Fourier series as

$$\mathbf{F}_i = F_{i1}\mathbf{e}_1^i + F_{i2}\mathbf{e}_2^i, \tag{1}$$

where

$$F_{i1} = \sum_{l=0}^{\infty} \{a_l^i \sin[l(\omega_m t + \phi_i)] + b_l^i \cos[l(\omega_m t + \phi_i)]\},$$

$$F_{i2} = \sum_{l=0}^{\infty} \{c_l^i \sin[l(\omega_m t + \phi_i)] + d_l^i \cos[l(\omega_m t + \phi_i)]\},$$

where  $\mathbf{e}_{1,2}^i$  are unit vectors that define the planet  $i$  local co-ordinates. Note that the bases  $\{\mathbf{e}_1^i, \mathbf{e}_2^i\}$  and  $\{\mathbf{i}, \mathbf{j}\}$  both rotate at the carrier speed and retain a fixed angular separation  $\psi_i$ .  $(\omega_m t + \phi_i)$  in equation (1) represents the phase angle of the  $i$ th planet in its tooth mesh.  $\phi_i$  is the initial phase angle of the  $i$ th planet mesh and is determined based on the planet positioning and the number of teeth on the sun gear. In one complete revolution of a planet gear center around the sun gear,  $Z_s$  tooth mesh cycles are completed. In other words, when a planet gear revolves by an angle of  $2\pi$  around the sun gear, the tooth mesh advances by a phase angle of  $2\pi Z_s$ . Accordingly, when a planet gear revolves by an angle of  $\psi_i$  around the sun gear, the phase angle by which the tooth mesh advances is

$$\phi_i = \psi_i Z_s, \tag{2}$$

where  $\psi_i$  is the initial positioning angle of the  $i$ th planet.

The forces acting on the sun gear from the  $i$ th planet mesh are evaluated in the carrier fixed  $\{\mathbf{i}, \mathbf{j}\}$  basis as

$$\mathbf{F}_i = F_{ix}\mathbf{i} + F_{iy}\mathbf{j}, \quad \begin{bmatrix} F_{ix} \\ F_{iy} \end{bmatrix} = \begin{bmatrix} \cos \psi_i & \sin \psi_i \\ -\sin \psi_i & \cos \psi_i \end{bmatrix} \begin{bmatrix} F_{i1} \\ F_{i2} \end{bmatrix}. \tag{3}$$

The net force acting on the sun gear through all  $N$  sun-planet meshes is then

$$\mathbf{F}_{sun} = F_x\mathbf{i} + F_y\mathbf{j} = \sum_{i=1}^N \{F_{ix}\mathbf{i} + F_{iy}\mathbf{j}\}. \tag{4}$$

Using equations (4), (3), (1), and (2), the net sun gear forces  $F_x$ ,  $F_y$  and their Fourier components  $F_x^l$ ,  $F_y^l$  are

$$F_x = \sum_{i=1}^N F_{ix} = \sum_{i=1}^N [\cos \psi_i F_{i1} + \sin \psi_i F_{i2}] = \sum_{l=0}^{\infty} F_x^l,$$

$$F_x^l = \sum_{i=1}^N \underbrace{[a_l^i \cos \psi_i \sin(l\omega_m t + lZ_s \psi_i) + b_l^i \cos \psi_i \cos(l\omega_m t + lZ_s \psi_i)]}_I$$

$$+ c_i^l \sin \psi_i \sin(l\omega_m t + lZ_s \psi_i) + d_i^l \sin \psi_i \cos(l\omega_m t + lZ_s \psi_i], \tag{5}$$

$$F_y = \sum_{i=1}^N F_{iy} = \sum_{i=1}^N [-\sin \psi_i F_{i1} + \cos \psi_i F_{i2}] = \sum_{l=0}^{\infty} F_y^l,$$

$$F_y^l = \sum_{i=1}^N [-a_i^l \sin \psi_i \sin(l\omega_m t + lZ_s \psi_i) - b_i^l \sin \psi_i \cos(l\omega_m t + lZ_s \psi_i) + c_i^l \cos \psi_i \sin(l\omega_m t + lZ_s \psi_i) + d_i^l \cos \psi_i \cos(l\omega_m t + lZ_s \psi_i)].$$

$F_x^l$  and  $F_y^l$  represent the  $l$ th harmonic components of the *net* sun gear forces from all planets; they are key elements in the subsequent development. The first term,  $I$ , of  $F_x^l$  in equation (5) takes the form

$$I = \sum_{i=1}^N a_i^l [\cos \psi_i \cos lZ_s \psi_i \sin l\omega_m t + \cos \psi_i \sin lZ_s \psi_i \cos l\omega_m t] \\ = \frac{1}{2} \sum_{i=1}^N a_i^l \{ [\cos(\psi_i(lZ_s + 1)) + \cos(\psi_i(lZ_s - 1))] \sin l\omega_m t + [\sin(\psi_i(lZ_s + 1)) + \sin(\psi_i(lZ_s - 1))] \cos l\omega_m t \}. \tag{6}$$

Similar expressions can be written for other terms of equation (5). The results obtained so far are valid for general spur planetary gear systems with arbitrarily spaced planets.

### 3.1. EQUALLY SPACED PLANETS

For systems with equally spaced planets the Fourier coefficients  $a_i^l, b_i^l, c_i^l, d_i^l$  in equation (1) are the same for each planet mesh, that is,  $a_i^l = a^l$  with similar expressions for the  $b_i^l, c_i^l, d_i^l$ . To justify this, the forces at one mesh (say, mesh  $i$ ) must equal those at another mesh (say, mesh  $j$ ) (with the exception of a time lag) if both the geometric configuration and mesh phase of all other planets with respect to planet  $i$  and  $j$  are identical. The geometric requirement is satisfied with the equal planet spacing

$$\psi_i = \frac{2\pi(i - 1)}{N}. \tag{7}$$

The mesh phase difference between the  $k$ th and  $i$ th planets is  $\Delta\phi_{ki} = \phi_k - \phi_i = Z_s(\psi_k - \psi_i)$ . The phase difference between planet  $i$  and all other planets relative to planet  $i$  are the same as the mesh phase differences between any other planet  $j$  and the corresponding planets relative to planet  $j$ . Thus, all planets see identical geometric configurations and relative mesh phases of the surrounding planets, and the mesh forces at all meshes must be the same (with the exception of a time lag captured by the phase differences). The finite element results reflect this conclusion, which is based solely on symmetry arguments.

Substitution of equation (7) into equation (6) yields

$$I = \frac{1}{2}a^l \sum_{i=1}^N \left\{ \cos \left[ \frac{2\pi(i-1)(lZ_s + 1)}{N} \right] + \cos \left[ \frac{2\pi(i-1)(lZ_s - 1)}{N} \right] \right\} \sin l\omega_m t + \left\{ \sin \left[ \frac{2\pi(i-1)(lZ_s + 1)}{N} \right] + \sin \left[ \frac{2\pi(i-1)(lZ_s - 1)}{N} \right] \right\} \cos l\omega_m t. \tag{8}$$

We define a new quantity  $k$  as

$$k = \text{mod} \left( \frac{lZ_s}{N} \right), \tag{9}$$

where  $\text{mod}(a/b)$  means the integer remainder of the integer division of  $a$  and  $b$ . Rearranging equation (8) with use of equation (9) gives

$$I = \frac{1}{2}a^l \sum_{i=1}^N \left\{ \left\{ \cos \left[ \frac{2\pi(i-1)(k+1)}{N} \right] + \cos \left[ \frac{2\pi(i-1)(k-1)}{N} \right] \right\} \sin l\omega_m t + \left\{ \sin \left[ \frac{2\pi(i-1)(k+1)}{N} \right] + \sin \left[ \frac{2\pi(i-1)(k-1)}{N} \right] \right\} \cos l\omega_m t \right\}. \tag{10}$$

The following identities hold for integer values of  $m$ :

$$\sum_{i=1}^N \cos \left[ \frac{2\pi(i-1)m}{N} \right] = \begin{cases} 0, & m/N \neq \text{integer} \\ N, & m/N = \text{integer} \end{cases},$$

$$\sum_{i=1}^N \sin \left[ \frac{2\pi(i-1)m}{N} \right] = 0. \tag{11}$$

With these identities, all terms in equation (10) reduce to zero for  $k \neq 1$  and  $N - 1$  and the first term of equation (5) vanishes. Similar operations reduce all other terms of  $F_x^l$  and  $F_y^l$  in equation (5) to zero for  $k \neq 1, N - 1$ . Hence, components  $F_x^l$  and  $F_y^l$  of the net force acting on the sun gear in the  $l$ th harmonic vanish for  $k \neq 1$  and  $N - 1$ . For  $k = 1$  or  $N - 1$ ,  $I$  in equation (10) and other terms in equation (5) do not vanish. In these cases, the  $l$ th harmonic of the net sun force is non-zero.

The net torque acting on the sun gear through the  $N$  sun-planet meshes is

$$T_{sun} = r_{sun} \sum_{i=1}^N F_{i2}. \tag{12}$$

Using equations (1) and (2),

$$T_{sun} = r_{sun} \sum_{i=1}^N \sum_{l=0}^{\infty} \{c_i^l \sin[l(\omega_m t + \phi_i)] + d_i^l \cos[l(\omega_m t + \phi_i)]\} = \sum_{l=0}^{\infty} T^l,$$

$$T^l = r_{sun} \sum_{i=1}^N [c_i^l \sin(l\omega_m t + lZ_s \psi_i) + d_i^l \cos(l\omega_m t + lZ_s \psi_i)], \tag{13}$$



TABLE 2

*Conditions for suppression of the lth mesh frequency harmonic of the net sun force and torque for a planetary gear system with equally spaced planets. The third column indicates which sun/ring/carrier responses occur and which mode types are excited/suppressed in the lth mesh frequency harmonic*

$k = \text{mod}(lZ_s/N)$	$l$ th Mesh frequency harmonic of the excitation on the sun/ring/carrier	Comments on dynamic response
0	$F_x^l, F_y^l = 0$ $T^l \neq 0$	Translational response/modes suppressed Rotational response/modes excited
1, $N - 1$	$F_x^l, F_y^l \neq 0$ $T^l \neq 0$	Translational response/modes excited Rotational response/modes suppressed
$k \neq 0, 1, N - 1$	$F_x^l, F_y^l = 0$ $T^l \neq 0$	Rotational and translational response/modes suppressed

where  $T^l$  is the  $l$ th harmonic of the net sun torque. Equation (13) is valid for general planetary gears with arbitrarily spaced planets. For equally spaced planets, substitution of equation (7) into equation (13) gives

$$\begin{aligned}
 T^l/r_{sun} = & \sum_{i=1}^N \left\{ \left[ c_i^l \cos \frac{2\pi(i-1)lZ_s}{N} - d_i^l \sin \frac{2\pi(i-1)lZ_s}{N} \right] \sin l\omega_m t \right. \\
 & \left. + \left[ c_i^l \sin \frac{2\pi(i-1)lZ_s}{N} + d_i^l \cos \frac{2\pi(i-1)lZ_s}{N} \right] \cos l\omega_m t \right\}. \tag{14}
 \end{aligned}$$

Recalling that  $c_i^l = c_l$ ,  $d_i^l = d_l$  and using equation (9), equation (14) gives

$$\begin{aligned}
 T^l/r_{sun} = & \left[ c^l \sum_{i=1}^N \cos \frac{2\pi(i-1)k}{N} - d^l \sum_{i=1}^N \sin \frac{2\pi(i-1)k}{N} \right] \sin l\omega_m t \\
 & + \left[ c^l \sum_{i=1}^N \sin \frac{2\pi(i-1)k}{N} + d^l \sum_{i=1}^N \cos \frac{2\pi(i-1)k}{N} \right] \cos l\omega_m t. \tag{15}
 \end{aligned}$$

With the identities of equation (11), the net torque acting on the sun gear in the  $l$ th harmonic vanishes for  $k \neq 0$ . The net sun torque has a non-zero  $l$ th harmonic for  $k = 0$ .

The ring and carrier forces and torques behave exactly as the sun. To see this, the absence of any net force on the sun in the  $l$ th harmonic implies there is no sun translation and thus no response in any translational modes at this harmonic. Because translational modes are the only modes involving ring or carrier translation, there is no ring or carrier translation in the  $l$ th harmonic. This implies that the  $l$ th harmonic of the net force on these components vanishes. Similar arguments based on rotational modes hold for torques and rotational responses. These conclusions can be obtained for the ring gear directly from a mesh force analysis like that conducted for the sun, but a carrier analysis involves the forces at the planet bearings.

The above findings, which are summarized in Table 2, lead to immediate conclusions for the response of equally spaced planet systems. The spectral content of the sun/ring/carrier

*translation* will contain only mesh frequency harmonics for which the net sun/ring/carrier force is non-zero, that is,  $k = 1$  or  $N - 1$ . Likewise, the sun/ring/carrier *rotation* will contain only harmonics for which the net sun/ring/carrier torque is non-zero, that is,  $k = 0$ . These conclusions explain the presence of all harmonics in the sun rotation and the absence of any sun translation for the example three planet system where  $k = \text{mod}(27l/3) = 0$  for any  $l$  [10]. The planet response contains all mesh frequency harmonics, in general, as the net force and torque on each planet in each harmonic is non-zero (Figure 3).

Vanishing of the  $l$ th harmonic of the net forces and torques on the sun, ring, and carrier has important implications for the excitation or suppression of resonant response. While one would expect resonance when  $l\omega_m = \omega_n$ , where  $\omega_n$  is a natural frequency, no resonance will be excited by the  $l$ th harmonic if (Table 2): (1)  $\omega_n$  corresponds to a translational mode and  $k \neq 1, N - 1$ ; (2)  $\omega_n$  corresponds to a rotational mode and  $k \neq 0$ ; or (3)  $\omega_n$  corresponds to a translational or a rotational mode and  $k \neq 0, 1, N - 1$ .

These rules correspond to the three cases depicted in Figure 4. They are consistent with Kahraman [4]. For the example three planet system where  $k = 0$  for any  $l$ , no resonances are excited for the translational modes. This is evident in the planet deflection (Figure 3) where resonances at  $f_1 = 780$  and  $f_5 = 2145$  Hz are absent. In contrast, rotational mode resonances are excited in all harmonics (Figure 3).

### 3.2. DIAMETRICALLY OPPOSED PLANETS

One can extend the prior analysis to address planetary gears with *unequally* spaced planets. Again, relationships between the Fourier coefficients for the forces acting on the sun gear through different planet meshes are essential. For instance, the four planet system in the example has diametrically opposed planets with  $\psi_3 = \psi_1 + \pi$  and  $\psi_4 = \psi_2 + \pi$ . As a result,  $a_3^l = a_1^l$  and  $a_4^l = a_2^l$  with similar relationships for the  $b_i^l$ ,  $c_i^l$ ,  $d_i^l$ . To justify this, consider the relative positions and mesh phases of planets with respect to planets 1 and 3. Notice that planets 2, 3, and 4 are positioned at angles  $\psi_2 - \psi_1$ ,  $\pi$  and  $\psi_2 - \psi_1 + \pi$ , respectively, relative to planet 1; planets 4, 1 and 2 have identical positions relative to planet 3. The mesh phase angles of the second, third and fourth planets relative to the first planet, obtained using equation (2), are  $Z_s(\psi_2 - \psi_1)$ ,  $Z_s\pi$ , and  $Z_s(\psi_2 - \psi_1 + \pi)$  respectively. The mesh phase angles of the fourth, first and second planets relative to the third planet are identical. Thus, planets 1 and 3 see the same geometric configurations and relative mesh phasing of the surrounding planets. Consequently, their mesh forces must be the same except for a time lag, and their Fourier coefficients are identical (e.g.,  $a_3^l = a_1^l$ ). Similar reasoning applies for the second and fourth planets (e.g.,  $a_4^l = a_2^l$ ). As with equally spaced planet systems, the finite element simulations confirm these results derived from symmetry arguments.

As a result, the first term of  $F_x^l$  in equation (5) reduces as follows:

$$\begin{aligned} I &= a_1^l [\cos \psi_1 \sin(l\omega_m t + lZ_s\psi_1) + \cos \psi_3 \sin(l\omega_m t + lZ_s\psi_3)] \\ &\quad + a_2^l [\cos \psi_2 \sin(l\omega_m t + lZ_s\psi_2) + \cos \psi_4 \sin(l\omega_m t + lZ_s\psi_4)] \\ &= a_1^l [\cos \psi_1 \sin(l\omega_m t + lZ_s\psi_1) + \cos(\psi_1 + \pi) \sin(l\omega_m t + lZ_s(\psi_1 + \pi))] \\ &\quad + a_2^l [\cos \psi_2 \sin(l\omega_m t + lZ_s\psi_2) + \cos(\psi_2 + \pi) \sin(l\omega_m t + lZ_s(\psi_2 + \pi))] \end{aligned}$$

$$\begin{aligned}
 &= a_1^l \cos \psi_1 [\sin(l\omega_m t + lZ_s \psi_1) - \sin(l\omega_m t + lZ_s \psi_1) \cos(lZ_s \pi)] \\
 &\quad + a_2^l \cos \psi_2 [\sin(l\omega_m t + lZ_s \psi_2) - \sin(l\omega_m t + lZ_s \psi_2) \cos(lZ_s \pi)] \\
 &= \left\{ \begin{array}{ll} 0, & lZ_s \text{ even} \\ 2a_1^l \cos \psi_1 \sin(l\omega_m t + lZ_s \psi_1) + 2a_2^l \cos \psi_2 \sin(l\omega_m t + lZ_s \psi_2), & lZ_s \text{ odd} \end{array} \right\}. \quad (16)
 \end{aligned}$$

Other terms of  $F_x^l, F_y^l$  reduce in a similar way. The  $l$ th harmonic of the net sun force vanishes for even values of  $lZ_s$ . For odd values of  $lZ_s$ , equation (16) and similar expressions for the other terms of equation (5) do not reduce to zero, and a non-zero net force acts in the  $l$ th harmonic. Reduction of the  $l$ th harmonic of the net sun torque (13) gives

$$\begin{aligned}
 T^l/r_{sun} &= c_1^l [\sin(l\omega_m t + lZ_s \psi_1) + \sin(l\omega_m t + lZ_s \psi_3)] \\
 &\quad + c_2^l [\sin(l\omega_m t + lZ_s \psi_2) + \sin(l\omega_m t + lZ_s \psi_4)] + d_i^l \text{ term} \\
 &= c_1^l [\sin(l\omega_m t + lZ_s \psi_1) + \sin(l\omega_m t + lZ_s \psi_1 + lZ_s \pi)] \\
 &\quad + c_2^l [\sin(l\omega_m t + lZ_s \psi_2) + \sin(l\omega_m t + lZ_s \psi_2 + lZ_s \pi)] + d_i^l \text{ term} \\
 &= \left\{ \begin{array}{ll} 2c_1^l \sin(l\omega_m t + lZ_s \psi_1) + 2c_2^l \sin(l\omega_m t + lZ_s \psi_2), & lZ_s \text{ even} \\ 0, & lZ_s \text{ odd} \end{array} \right\} + d_i^l \text{ term}, \quad (17)
 \end{aligned}$$

where only the first term is shown explicitly but the  $d_i^l$  term reduces in the same way. The  $l$ th harmonic of the net sun torque vanishes for odd values of  $lZ_s$  but not for even values of  $lZ_s$ . Because diametrically opposed planet systems also have only translational, rotational, and planet modes [8], reasoning analogous to that for equally spaced planets shows that net ring and carrier forces and torques have identical spectral content as the sun. The above results are summarized in Table 3.

The foregoing development extends to general planetary gears with  $M = N/2$  pairs of planets on diametral axes. In this case,  $\psi_{M+i} = \psi_i + \pi$  for  $1 \leq i \leq M$ . For such systems, the sun, ring, and carrier translation have response only in the mesh frequency harmonics where  $lZ_s$  is odd; sun, ring, and carrier rotation have response only in the mesh frequency harmonics where  $lZ_s$  is even. As with equally spaced planet systems, resonances in certain modes are suppressed for some mesh frequency harmonics. The rules are (Table 3): (1) translational mode resonances are excited in the  $l$ th harmonic if  $lZ_s$  is odd and suppressed if  $lZ_s$  is even, and (2) rotational mode resonances are excited in the  $l$ th harmonic if  $lZ_s$  is even and suppressed if  $lZ_s$  is odd. Considering Figure 2, the presence of odd harmonic resonances in the translational modes  $f_1$  and  $f_6$  and the absence of even harmonic resonances in these modes are examples of the first rule. Resonances for the rotational mode  $f_2$  in Figure 2 demonstrate the second rule.

#### 4. DISCUSSION AND SUMMARY

Planet phasing provides an effective means to reduce planetary gear vibration. A significant advantage is its cost-effectiveness as no additional manufacturing processes are needed. The simple rules (Tables 2 and 3) for when a given type of mode (translational or rotational) is excited by a particular mesh frequency harmonic are derived solely from

TABLE 3

*Conditions for suppression of the  $l$ th mesh frequency harmonic of the net sun force and torque for a planetary gear system with pairs of diametrically opposed planets. The third column indicates which sun/ring/carrier responses occur and which mode types are excited/suppressed in the  $l$ th mesh frequency harmonic*

$lZ_s$	$l$ th Mesh frequency harmonic of the excitation on the sun/ring/carrier	Comments on dynamic response
Even	$F_x^l, F_y^l = 0$ $T^l \neq 0$	Translational response/modes suppressed Rotational response/modes excited
Odd	$F_x^l, F_y^l \neq 0$ $T^l = 0$	Translational response/modes excited Rotational response/modes suppressed

system symmetries that imply distinct relationships between the forces at the sun-planet and ring-planet meshes. No assumptions are made on the use of static transmission error to model the dynamic excitation. Additionally, the results are independent of any analytical model. They apply for general epicyclic spur gears. The phenomena associated with phasing are evident in two example problems based on a dynamic finite element/contact mechanics simulation. A distinction of this simulation compared to prior works is that it does not impose the phasing predictions on the response by assuming particular spectral content in the dynamic excitations or equal forces at the multiple meshes. In this sense, the simulation genuinely verifies the phasing analysis without recourse to any analytical assumptions.

The ability to suppress particular resonance conditions is particularly important. The conditions in Tables 2 and 3 to suppress translational and rotational mode resonances are easily achieved. For example, diametrically opposed planet spacing with any number of planets suppresses either translational or rotational mode resonances (but not both) in any given mesh frequency harmonic  $l$ . For such systems with an even number of sun gear teeth, *all* translational mode resonances are suppressed in *all* harmonics; no rotational mode resonances are suppressed. With an odd number of sun gear teeth, translational mode resonances are suppressed for all even mesh frequency harmonics, and rotational mode resonances are suppressed for all odd mesh frequency harmonics. More suppression is possible in equally spaced planet systems, where at least one of the translational or rotational mode resonances (and both if  $k \neq 0, 1, N - 1$ ) are suppressed for *any* given mesh frequency harmonic  $l$ . For example, if  $Z_s/N$  is an integer,  $k = 0$  and *all* translational mode resonances are suppressed in all harmonics. *For both planet spacing conditions, potential resonances in at least half of the mesh frequency harmonics are suppressed without any attempt to optimize the phasing.*

Planet phasing can not suppress all potential resonances. It may be most effective for narrow speed ranges as suppression of all resonances in a wide mesh frequency range is not feasible. Designers may also base their phasing choices on which type of resonant response (translational or rotational mode) is considered most damaging for noise, tooth loads, bearing forces, etc.

The conditions in Tables 2 and 3 imply more than the suppression of resonances in a given harmonic. They indicate when the sun, ring, and carrier translation/rotation are absent in a given mesh frequency harmonic. For example, results in reference [10] show the absence of even harmonics in the sun translation and the absence of odd harmonics in the sun rotation for the diametrically opposed four planet system. The ring and carrier have the same character.

## ACKNOWLEDGMENT

The author thanks T. L. Krantz of the Army Research Lab for helpful discussions and advice throughout the work. V. Agashe and S. M. Vijayakar generated the simulation results. This material is based on work supported by the NASA Glenn Research Center under grant NAG-1979 and the U.S. Army Research Office under grant DAAD19-99-1-0218.

## REFERENCES

1. R. G. SCHLEGEL and K. C. MARD 1967 *ASME Design Engineering Conference* New York, ASME paper 67-DE-58. Transmission noise control-approaches in helicopter design.
2. D. L. SEAGER 1975 *Journal of Mechanical Engineering Science* **17**, 293–298. Conditions for the neutralization of excitation by the teeth in Epicyclic Gearing.
3. W. E. PALMER and R. R. FUEHRER 1977 *Earthmoving Industry Conference* Peoria, SAE paper 770561. Noise control in planetary transmissions.
4. A. KAHRAMAN 1994 *Journal of Mechanical Design* **116**, 713–720. Planetary gear train dynamics.
5. A. KAHRAMAN and G. W. BLANKENSHIP 1994 *Proceedings of International Gearing Conference* Newcastle, 99-104. Planet mesh phasing in epicyclic gear sets.
6. R. L. PLATT and R. D. LEOPOLD 1996 *VDI Berichte* **1230**, 793–807. A study on helical gear planetary phasing effects on transmission noise.
7. J. LIN and R. G. PARKER 1999 *Journal of Vibration and Acoustics* **121**, 316–321. Analytical characterization of the unique properties of planetary gear free vibration.
8. J. LIN and R. G. PARKER 2000 *Journal of Sound and Vibration* **233**, 921–928. Structured vibration characteristics of planetary gears with unequally spaced planets.
9. T. L. KRANTZ 1992 *NASA Technical Memorandum* 105651, AVSCOM Technical Report 91-C-038, 1-8. Gear tooth stress measurements of two helicopter planetary stages.
10. R. G. PARKER, V. AGASHE, and S. M. VIJAYAKAR 2000 *Journal of Mechanical Design* **122**, 305–311. Dynamic response of a planetary gear system using a finite element/contact mechanics model.